View metadata, citation and similar papers at core.ac.uk

brought to you by CORE

provided by Archivio istituzionale della ricerca - Politecnico di Milano

ChemComm

COMMUNICATION

Pulsed laser deposition of porous N-carbon supported cobalt (oxide) thin films for highly efficient oxygen evolution

Received 00th January 20xx,
Accepted 00th January 20xx

DOI: 10.1039/x0xx00000x

www.rsc.org/

Bita Bayatsarmadi[a], Yao Zheng[a], Carlo Spartaco Casari[b,*], Valeria Russo[b] and Shi-Zhang Qiao[a,*]

Identifying efficient non-precious metal catalysts for oxygen evolution reaction (OER) remains a great challenge. Here we report robust cobalt (oxide) nanoparticles deposited on porous nitrogen-doped carbon (N-carbon) film prepared by pulsed laser deposition under a reactive background gas which exhibit highly efficient OER performance with low overpotential and high stability.

The global energy crisis has prompted intense research into the development of various types of sustainable energy conversion and storage systems.[1] Splitting water is widely considered to be a critical step toward efficient renewable energy production, storage and usage. One of the major hurdles in making water electrolysis commercially more viable is the low efficiency of the anodic oxygen evolution reaction (OER) and the high cost of conventional OER catalysts such as IrO_2 and RuO_2.[2] Inexpensive and durable "noble metal-free" electrocatalysts such as non-precious metal and metal-free nanostructures, as well as their hybrids, have received much attention recently.[3] Among different non-precious metals, cobalt-based materials are promising OER catalysts, however, the easy accumulation and low conductivity of pure cobalt oxides decreases the available active sites and limits charge transport during the oxidation process.[4] On the other hand, various carbon-based materials feature unique advantages due to their tunable molecular structures, abundance, and strong tolerance to acid/alkaline environments. The interplay between carbon and cobalt oxide nanoparticles can modify the overall physicochemical and electronic structures which make the resultant composites highly competitive to traditional cobalt-based electrocatalysts.[5]

Despite recent progress in developing non-precious metal (specifically cobalt) based hybrid materials, new OER electrocatalysts with low overpotentials and long-term stability are still needed. To overcome these challenges, synthesis techniques are required which ensure high control and tunability of morphology, structure and composition of multi-component materials. Physical vapour deposition (PVD) techniques allow high purity and control in the fabrication of coatings and thin films. In this context, pulsed laser deposition (PLD) is particularly versatile in the tuning of properties of deposited materials[6] which is based on ablating a target material by laser pulses to produce plasma of ejected species that can be deposited onto a substrate. The control of the ablation process permits the tuning of the growth mode and properties of the deposited films over a wide range.[7]

Herein, we demonstrate highly porous N-carbon film supported cobalt (oxide) nanoparticles prepared by two-step pulsed laser deposition under a reactive background gas at room temperature as a highly efficient and durable OER electrocatalyst in strongly alkaline electrolytes. The obtained film exhibits overpotential of 349.0 mV to achieve a catalytic current density of 10 $mAcm^{-2}$ toward OER. A detailed physicochemical characterization of this material further confirms that its superior performance originates from the porous structure and high conductivity of N-carbon and the synergetic effect of the cobalt (oxide) nanoparticles and the N-carbon films.

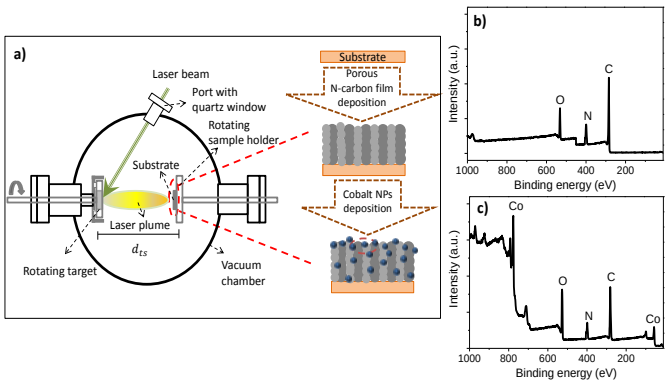

Figure 1- (a) Schematic illustration of the two step synthesis process of cobalt (oxide) nanoparticles deposited on porous N-carbon film $(Co(Ox)_P@PNC)$ and XPS survey of (b) first step product (PNC) and (c) final product $(Co(Ox)_P@PNC)$.

[a] School of Chemical Engineering, University of Adelaide, Adelaide SA 5005 Australia. Email: s.qiao@adelaide.edu.au
[b] Department of Energy, Politecnico di Milano, via Ponzio 34/3, 20133 Milano, Italy. Email: carlo.casari@polimi.it

Electronic Supplementary Information (ESI) available: See DOI: 10.1039/x0xx00000x

Please do not adjust margins

Please do not adjust margins

The two step fabrication process of cobalt (oxide) nanoparticles deposited on porous N-carbon films (denoted as $Co(Ox)_P$@PNC; subscript P is the background gas pressure in Pa) is illustrated in Figure 1a. In the first step, porous N-carbon (PNC) films were deposited on substrates (Silicon and Copper foil) by PLD with pulse energy of 200 mJ (λ = 532 nm) at room temperature using a highly pure graphite target under N_2 gas flow. Laser pulses ablate the target ejecting material in a plasma plume in the presence of a background gas within the pressure range of 10 to 100 Pa to tune morphology, structure and composition of the deposited film. The X-ray photoelectron spectroscopy (XPS) survey indicates the chemical composition of PNC films contains C, O and N (Figure 1b). By controlling deposition parameters (e.g. background gas pressure, target-to-substrate distance and deposition time), thin films with various porous structures and specific surface area were formed (Figure S1). Such porous structures are favourable for the deposition of metal nanoparticles in second step, as the latter could easily go through and stay on the surface or side walls of the porous carbon network.

Ablation in a reactive atmosphere (high purity N_2 gas) was performed to incorporate nitrogen into the carbon framework and create C-N moieties to enhance the electrical conductivity. Following this, cobalt nanoparticles were deposited on PNC films (operating as the substrate) using an ultra-pure cobalt target with a nitrogen background gas pressure of 50 Pa to form $Co(Ox)_{50}$@PNC. As shown in Figure 1c, the XPS survey of $Co(Ox)_{50}$@PNC confirms the successful incorporation of cobalt species into the N-carbon framework (See Experimental section for details). The cobalt deposition time was calculated based on the desired amount of cobalt in final product (e.g. 10 at %) using quartz crystal microbalance (QCM) measurements.

The morphology and nanostructures of the synthesized materials were investigated by scanning electron microscopy (SEM) and transmission electron microscopy (TEM). The SEM top view image of the PNC films (Figure 2a) shows complete coverage of the surface by a porous carbon film formed by fine N-carbon nanoparticles at low kinetic energy.[8] The SEM cross-sectional image (inset of Figure 2a) demonstrates a thin film with thickness of about 210 nm and highly porous columnar nanostructure. As shown in Figure S2, the surface morphology of deposited N-carbon films is getting opener with increasing background gas pressure from 10 to 100 Pa during the deposition process. The cross-sectional SEM images (insets of Figure S2) show that the films formed at lower gas pressures (i.e. 10 and 30 Pa) are more compact while films formed at higher pressures (i.e. 50 and 100 Pa) are more porous with mean pore size of approximately 10 nm. Notably, Figure S2d (film deposited at 100 Pa) exhibits an irregular and highly disordered structure which barely covers the substrate and has poor film-substrate adhesion. From these results, the PNC film deposited at 50 Pa represents the optimal condition for the deposition of low density N-carbon foam with a porous and uniform structure which is favourable as a substrate for cobalt (oxide) deposition. Hence, the deposition parameters were carefully tuned to ensure that the subsequent deposition of cobalt did not damage or alter the morphology of the porous

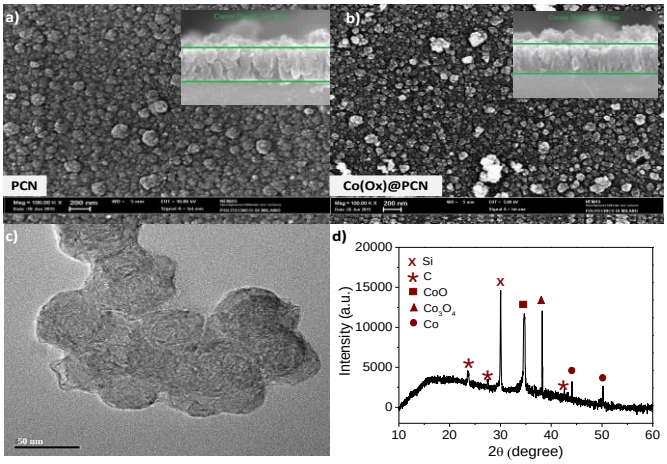

Figure 2- Top view SEM image and (insets) cross-sectional image of (a) PNC film deposited at 50 Pa and (b) $Co(Ox)_{50}$@PNC at 50 Pa, (c) TEM image of $Co(Ox)_{50}$@PNC and (d) XRD pattern of $Co(Ox)_{50}$@PNC .

N-carbon support layer, as shown in Figure 2b, where is clearly seen that there is no change on surface and cross section of film compared to that of PNC. The magnified TEM image (Figure 2c) shows the $Co(Ox)_{50}$@PNC films are the aggregation and assembly of nanoparticles in a cauliflower-like fashion with an average diameter of about 50 nm. Note that there is no sign for the presence of large bulk cobalt species which confirms the homogenous ablation of the cobalt target. Figure S3 displays the HR-TEM images of $Co(Ox)_p$@PNC films with cobalt deposition at different background gas pressures ranging from 1 to 50 Pa. It is clearly seen that the cobalt nanoparticles form compact clusters at lower gas pressures (e.g. 1 and 10 Pa), while porous structured cobalt nanocrystals are embedded within the N-carbon framework at gas pressure of 50 Pa, which could be more favourable for catalytic activity toward the OER.

The X-ray diffraction (XRD) pattern of the synthesized material corresponds well to what is expected for nanocrystalline $Co(Ox)_{50}$@PNC (Figure 2d), which shows the existence of metallic Co and cobalt oxides including CoO and Co_3O_4.[9] The XRD pattern also exhibits a peak at ca. 24° and 27.5° which is attributed to the (002) facets of graphitic carbon and the stacking peak of pi-conjugated layers for graphitic materials.[10] It is also shown a weak peak at 42.5° which confirms the presence of the (100) plane of disordered amorphous carbon.

Figure 3a represents a typical Raman spectrum of $Co(Ox)_{50}$@PNC, demonstrating a sharp peak at 675 cm^{-1} assigned to cobalt oxide[11] (the other sharp peak at 521 cm^{-1} is a silicon signal coming from the substrate) and a distinct large peak with a shoulder in the range of 1300-1600 cm^{-1} (G-D region). The shape of this large peak indicates that carbon is mostly in its amorphous form.[12] In order to identify the G and D peak properties (position, width and relative intensities), the Raman spectra were then analysed by fitting a Lorentzian to the D peak and a Breit-Wigner-Fano (BWF) line shape to the G peak. The best deconvolution of the peak at G-D region (inset of Figure 3a) shows two prominent broad G(1575 cm^{-1}) and D

 This journal is © The Royal Society of Chemistry 2016

Please do not adjust margins

Please do not adjust margins

(1345 cm^{-1}) bands which represent the crystallinity and disorder

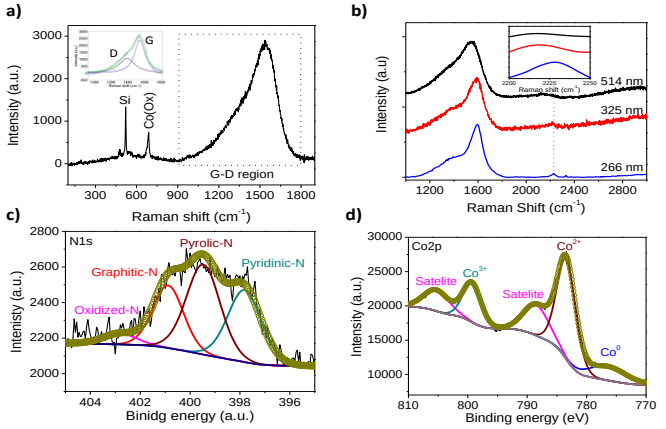

Figure 3- (a) Raman spectrum of $Co(Ox)_{50}$@PNC film, (b) Raman spectra of $Co(Ox)_{50}$@PNC film for different laser type (wavelength range), (c) High-resolution N1s spectrum and (d) High-resolution Co2p spectrum of $Co_{50}(Ox)$@PNC film.

of sp^2 carbon materials, respectively.[12] Notably, substitution of carbon atoms by other species (i.e nitrogen) is reasonably accompanied by the introduction of defects into the carbon network which can reflect on D band to G band intensity ratio (I_D/I_G).[13] Typical values of about 0.5 for the I_D/I_G ratio (Figure S4) together with the G position at about 1575 cm^{-1} are compatible with amorphous sp^2 carbon.[14] Figure 3b displays the Raman spectra of $Co(Ox)_{50}$@PNC at three different excitation wavelengths (i.e. 266, 325 and 514 nm) in order to confirm the C-N formation. A distinct peak at about 2200 cm^{-1}, which can be attributed to sp^1 bonded C-N groups, is clearly visible for 266 nm excitation, whilst it is barely detectable at 325 and 514 nm excitations. The enhancement of the peak assigned to C-N groups during UV excitation occurs due to their π-π* band gap which is only resonant for UV excitation.[15] As shown in Figure S5, the absence of the C-N peak at about 2200 cm^{-1} for $Co(Ox)_{50}$@PC confirms the introduction of nitrogen by ablation under reactive (nitrogen) atmosphere. By studying the cobalt oxide Raman peaks (Figure S6), it is clearly seen that the Raman active peak assigned to cobalt oxide slightly shifts and becomes weaker in samples deposited in lower nitrogen gas pressures. This might be attributed to the presence of cobalt (oxide) nanostructures with a different degree of structural order. Hence, the deposition of small cobalt nanoclusters may result in a better interconnection of cobalt with C-N species with an improved electrical conductivity.[16] Moreover, the lower cobalt (oxide) peak intensity at $Co(Ox)_{50}$@PNC compared to that of $Co(Ox)_{50}$@PC (with equal cobalt concentration) indicates that cobalt oxides are partially surrounded by some graphitic carbon layers, which is favourable for electrocatalyst stability.[17]

As the nitrogen atoms (structural defects) are an important component of $Co(Ox)_{50}$@PNC, the nitrogen bonding configurations were further studied by XPS spectrum. As shown in Figure 3c, the N1s spectrum comprises three main peaks located at about 397.8, 399.6 and 400.9 eV which corresponds to pyridinic, pyrrolic and graphitic nitrogen, respectively. Additionally, the wide peak present at about 402.7 eV is assigned to oxidized-nitrogen species.[18] It should be noted that the presence of graphitic nitrogen species confirms the substitution of some carbon for nitrogen atoms in the structure of $Co(Ox)_{50}$@PNC, which is believed to participate as the active sites.[19] Moreover, the existence of pyridinic and pyrrolic nitrogen is beneficial in improving conductivity of the carbon framework due to contribution of their p-conjugated system with a pair of p-electrons.[20] This successful incorporation of cobalt into the N-carbon framework was further revealed by Co 2p XPS spectrum (Figure 3d). The best deconvolution of Co 2p profile was achieved under the assumption of five peaks, indicating the existence of Co^0, Co^{2+}, Co^{3+} and their shake-up satellites. It should be noted that peaks with binding energies of 782.2 and 796.9 eV correspond to oxygen-coordinated metals (CoO and Co_3O_4) and the peak at 778.2 eV is attributed to Co^0.[21] By comparing binding energies of the peaks assigned to pure Cobalt oxides (~780.1 and 791.9 eV), the close assembly and strong interaction between oxygen-coordinated cobalt species and carbon is confirmed which results in the impaired electron density of Co atoms in $Co(Ox)_{50}$@PNC films.[22]

The OER electrocatalytic activity of the synthesised electrocatalysts was evaluated in a standard three-electrode system in an N_2-saturated 1.0 M KOH solution (Figure S7). The OER performance of $Co(Ox)_{50}$@PNC, $Co(Ox)_{50}$@PC and metal-free PNC films was tested using linear sweep voltammetry (LSV; Figure 4a). Remarkably, the $Co(Ox)_{50}$@PNC film can afford a current density of 10 $mAcm^{-2}$ at a small overpotential of 349 mV which is smaller than those of $Co(Ox)_{50}$@PC (387 mV), commercial IrO_2/C (462 mV), and metal-free PNC (maximum achieved current density of 7.5 $mAcm^{-2}$ at 576 mV). It is also comparable to the best reported carbon supported Co-based OER catalysts.[23] The OER kinetics of the above catalysts were studied by plotting their Tafel curves (Figure 4b). The resulting Tafel slopes are found to be 75.3, 84.1 and 103.8 $mVdec^{-1}$ for $Co(Ox)_{50}$@PNC, $Co(Ox)_{50}$@PC and PNC respectively, implying the critical role of cobalt (oxide) and nitrogen species in the

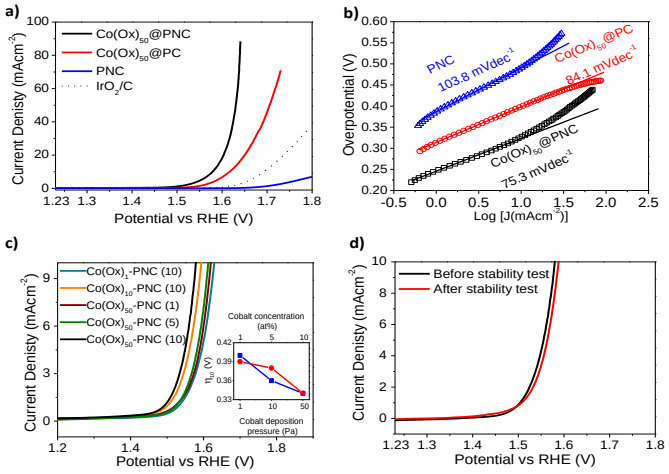

Please do not adjust margins

Please do not adjust margins

Figure 4- (a) OER polarization curve of $Co(Ox)_{50}$@PNC, $Co(Ox)_{50}$@PC, metal-free PNC and benchmarked IrO_2/C samples in 1.0 M KOH solution and (b) Corresponding OER Tafel plots of $Co(Ox)_{50}$@PNC, $Co(Ox)_{50}$@PC, metal-free PNC, (c) OER polarization curves and (inset of c) OER overpotential plots to reach a current density of 10 $mAcm^{-2}$ for $Co(Ox)_P$@PNC films at different cobalt deposition pressures and different cobalt concentrations at background gas pressure of 50 Pa in 1.0 M KOH solution and (d) OER polarization curves of $Co(Ox)_{50}$@PNC before and after stability test.

OER activity of these materials.[24] The $Co(Ox)_{50}$@PNC composite exhibits the smallest Tafel slope, even smaller than those of the best reported carbon supported Co-based OER catalysts, demonstrating the outstanding intrinsic OER kinetics of $Co(Ox)_{50}$@PNC. As shown in Figure 4c, the overpotential (η_{10} at a current density of 10 $mAcm^{-2}$) decreases for samples fabricated at greater background gas pressures during cobalt deposition process. This might be attributed to the formation of crystalline cobalt (oxide) at higher pressures which could possibly increase the interaction of cobalt species with the N-carbon structure. Moreover, a rise in the cobalt concentration (i.e 1, 5 and 10 at %) results in decreasing the overpotential which could be due to presence of a greater number of accessible cobalt (oxide) active sites towards oxygen evolution.

The stability of catalysts toward OER is also important for application of these catalysts in actual devices. Thus, a 24 h chronoamperometric test (Figure S8) of $Co(Ox)_{50}$@PNC was conducted which exhibited only an 8 mV increase in overpotential required to achieve a catalytic current density of 10 mA cm^{-2}. This excellent stability also demonstrates the potential of using $Co(Ox)_{50}$@PNC films as an efficient and stable OER catalyst (Figure 4d).

The above discussions indicate that the remarkable OER catalytic activity of $Co(Ox)_{50}$@PNC arises from its tuned Co^{2+} content, when compared to its nitrogen-free counterpart. This can be attributed to the strong interaction and synergetic effect of cobalt (oxide) nanoparticles with N-carbon films (as evidenced by TEM, Raman and XPS) and highly improved conductivity and charge transfer capability, which are favourable toward OER activity and stability. Last but not least, the direct growth of active materials on the conductive Cu foil can greatly enhance the electron transport and adhesion between porous films and substrates, promote the structural stability for long-term usage, and avoid utilization of polymeric binders and extra conductive additives, consequently reducing the dead volume and undesirable interface in the electrode.[25]

In conclusion, $Co(Ox)_{50}$@PNC films were successfully developed via a two-step pulsed laser deposition technique. The synthesised material behaves as an efficient OER electrocatalyst and has superior activity in 1.0 M KOH electrolyte. The excellent catalytic activity of $Co(Ox)_{50}$@PNC films could be attributed to the surrounding N-carbon framework and it was found that a higher ratio of Co^{2+}/Co^{3+} yields better catalytic activity towards the OER. Transport of reactants and products involved in electrochemical reactions was also facilitated by the porous structure of the material. Additionally, the carbon framework, comprising carbons adjacent to cobalt (oxide) nanoparticles, increases catalytic sites and prevents the aggregation or dissolution of nanoparticles. Together with the combined mutual effects of each structural component, this $Co(Ox)_{50}$@PNC OER catalyst outperforms most of the reported earth-abundant OER catalysts in activity and stability.

This work is financially supported by the Australian Research Council (ARC) through the Discovery Project programs (DP130104459, DP140104062, DP160104866).

Notes and references

1. S. Chu and A. Majumdar, *Nature*, 2012, **488**, 294.
2. J. L. Fillol, Z. Codolà, I. Garcia-Bosch, L. Gómez, J. J. Pla and M. Costas, *Nat Chem*, 2011, **3**, 807.
3. a) J. Lai, S. Li, F. Wu, M. Saqib, R. Luque and G. Xu, *Energy Environ. Sci.*, 2016, **9**, 1210; b) Y. Sun, Q. Wu and G. Shi, *Energy Environ. Sci.*, 2011, **4**, 1113; c) Y. Zhang, B. Cui, O. Derr, Z. Yao, Z. Qin, X. Deng, J. Li and H. Lin, *Nanoscale*, 2014, **6**, 3376.
4. X. Zou, A. Goswami and T. Asefa, *J. Am. Chem. Soc.*, 2013, **135**, 17242.
5. a) D. Kong, H. Wang, Z. Lu and Y. Cui, *J. Am. Chem. Soc.*, 2014, **136**, 4897; b) M. Shen, C. Ruan, Y. Chen, C. Jiang, K. Ai and L. Lu, *ACS Appl Mater Inter*, 2015, **7**, 1207.
6. a) S. C. Carlo and B. AndreaLi, *Oxide Nanostructures*, Pan Stanford Publishing, 2014, DOI:10.1201/b15633-3, pp. 99; b) P. Gondoni, P. Mazzolini, V. Russo, A. Petrozza, A. K. Srivastava, A. Li Bassi and C. S. Casari, *Sol. Energ. Mat. Sol. Cells*, 2014, **128**, 248.
7. D. Cattaneo, S. Foglio, C. S. Casari, A. Li Bassi, M. Passoni and C. E. Bottani, *Surf. Sci.*, 2007, **601**, 1892.
8. P. M. Ossi and A. Miotello, *Carbon*: The Future Material for Advanced Technology Applications, eds. G. Messina and S. Santangelo, Springer Berlin Heidelberg, Berlin, Heidelberg, 2006, DOI: 10.1007/11378235_18, pp. 359.
9. Y. Su, Y. Zhu, H. Jiang, J. Shen, X. Yang, W. Zou, J. Chen and C. Li, *Nanoscale*, 2014, **6**, 15080.
10. F. Dong, M. Ou, Y. Jiang, S. Guo and Z. Wu, *Ind. Eng. Chem. Res*, 2014, **53**, 2318.
11. Y. Li, W. Qiu, F. Qin, H. Fang, V. G. Hadjiev, D. Litvinov and J. Bao, *J. Phys. Chem. C*, 2016, **120**, 4511.
12. A. Zani, D. Dellasega, V. Russo and M. Passoni, *Carbon*, 2013, **56**, 358.
13. K. Kobayashi, R. Kitaura, Y. Kumai, Y. Goto, S. Imagaki and H. Shinohara, *Carbon*, 2009, **47**, 722.
14. A. C. Ferrari and J. Robertson, *Phys. Rev. B*, 2000, **61**, 14095.
15. A. C. Ferrari, S. E. Rodil and J. Robertson, *Diamond Relat. Mater.*, 2003, **12**, 905.
16. D. Gallant, M. Pézolet and S. Simard, *J. Phys. Chem. B*, 2006, **110**, 6871.
17. H. Jin, J. Wang, D. Su, Z. Wei, Z. Pang and Y. Wang, *J. Am. Chem. Soc.*, 2015, **137**, 2688.
18. Z.-H. Sheng, L. Shao, J.-J. Chen, W.-J. Bao, F.-B. Wang and X.-H. Xia, *ACS Nano*, 2011, **5**, 4350.
19. G. Wu, C. M. Johnston, N. H. Mack, K. Artyushkova, M. Ferrandon, M. Nelson, J. S. Lezama-Pacheco, S. D. Conradson, K. L. More, D. J. Myers and P. Zelenay, *J. Mater. Chem.*, 2011, **21**, 11392.
20. B. Kumar, M. Asadi, D. Pisasale, S. Sinha-Ray, B. A. Rosen, R. Haasch, J. Abiade, A. L. Yarin and A. Salehi-Khojin, *Nat Commun*, 2013, **4**, 2819.
21. Y. Chen, S. Zhao and Z. Liu, *Phys. Chem. Chem. Phys.,* 2015, **17**, 14012.
22. N. Weidler, S. Paulus, J. Schuch, J. Klett, S. Hoch, P. Stenner, A. Maljusch, J. Brotz, C. Wittich, B. Kaiser and W. Jaegermann, *Phys. Chem. Chem. Phys.*, 2016, **18**, 10708.
23. a) Y. Liang, Y. Li, H. Wang, J. Zhou, J. Wang, T. Regier and H. Dai, *Nat. Mater.*, 2011, **10**, 780; b) S. Mao, Z. Wen, T. Huang, Y. Hou and J. Chen, *Energy Environ. Sci.*, 2014, **7**, 609.

 This journal is © The Royal Society of Chemistry 2016

Please do not adjust margins

Please do not adjust margins

24. Y. Hou, J. Li, Z. Wen, S. Cui, C. Yuan and J. Chen, *Nano Energy*, 2015, **12**, 1.
25. D. U. Lee, J.-Y. Choi, K. Feng, H. W. Park and Z. Chen, *Adv. Energy Mater.*, 2014, **4**, 5.

This journal is © The Royal Society of Chemistry 2016

Please do not adjust margins